Biol. Cybern. 87, 416–427 (2002)
DOI 10.1007/s00422-002-0359-5

Biological Cybernetics

Spike-timing dependent synaptic plasticity: a phenomenological framework

Werner M. Kistler

Department of Neuroscience, Faculty of Medicine and Health Sciences, Erasmus University Rotterdam, The Netherlands

Received: 23 January 2002 / Accepted: 28 March 2002

Abstract. In this paper a phenomenological model of spike-timing dependent synaptic plasticity (STDP) is developed that is based on a Volterra series-like expansion. Synaptic weight changes as a function of the relative timing of pre- and postsynaptic spikes are described by integral kernels that can easily be inferred from experimental data. The resulting weight dynamics can be stated in terms of statistical properties of pre- and postsynaptic spike trains. Generalizations to neurons that fire two different types of action potentials, such as cerebellar Purkinje cells where synaptic plasticity depends on correlations in two distinct presynaptic fibers, are discussed.

We show that synaptic plasticity, together with strictly local bounds for the weights, can result in synaptic competition that is required for any form of pattern formation. This is illustrated by a concrete example where a single neuron equipped with STDP can selectively strengthen those synapses with presynaptic neurons that reliably deliver precisely timed spikes at the expense of other synapses which transmit spikes with a broad temporal distribution. Such a mechanism may be of vital importance for any neuronal system where information is coded in the timing of individual action potentials.

1 Introduction

Many interesting properties of neuronal networks arise from the intricate interplay of neuronal activity and synaptic plasticity. Synaptic coupling strengths control neuronal activity patterns and, vice versa, neuronal activity influences synaptic efficacies. There are multiple notions of neuronal activity and the proper choice of notion is intimately related to the question of how information in the brain is coded and processed. In order to obtain a coherent picture it is necessary to employ the same notion for the description of neuronal and synaptic dynamics. A description of neurons in terms of their (time-averaged) firing rate, for example, implies that changes of synaptic efficacies should be given solely as a function of pre- and postsynaptic firing rate. This description can account for results from experiments that use brief high frequency stimulation of presynaptic neurons to induce use-dependent alterations of synaptic strength as in the classical experiments on hippocampal long-term potentiation (LTP) (Bliss and Lomo 1970). On the other hand, it is known that information can be coded in the firing time of individual action potentials (Carr 1993). In order to obtain *meaningful* modifications of the network connectivity it has been concluded that synaptic plasticity should depend on the relative timing of pre- and postsynaptic action potentials at a millisecond time scale (Gerstner and van Hemmen 1994; Gerstner et al. 1996). A few years ago, *spike-timing dependent synaptic plasticity* (STDP) was found experimentally (Markram et al. 1997; Bell et al. 1997; Lev-Ram et al. 1997; Bi and Poo 1998).

The organization of the present paper is as follows. In Sect. 2 a generic model for STDP is introduced. No attempt is made to describe underlying bio-physical mechanisms such as membrane potential, transmitter release, and intra-cellular calcium dynamics. Instead, a purely phenomenological approach is adopted assuming that synaptic weight changes are fully determined by the set of pre- and postsynaptic firing times. Generalizations to neurons that fire two different types of action potentials, such as cerebellar Purkinje cells where synaptic plasticity depends on correlations in two distinct presynaptic fibers, are discussed. The resulting weight dynamics is analyzed in Sect. 3. In Sect. 4 a concrete example is studied which shows that an asymmetric learning rule can selectively strengthen those synapses that reliably transmit precisely timed spikes. Bounds for the synaptic weights result in a competition so that synapses that transmit less precisely timed spikes are weakened. Such a mechanism can be of great importance for any neuronal system where information is coded in the timing of individual action potentials.

Correspondence to: W.M. Kistler
(e-mail: kistler@anat.fgg.eur.nl
Fax: +31 10 408 5459)

2 A phenomenological model for STDP

In the following sections, we develop a phenomenological model for STDP. We assume that apart from an activity-independent weight decay *all* changes are triggered by pre- or postsynaptic action potentials. For the sake of simplicity – and for want of detailed knowledge – we take weight changes to be instantaneous, i.e., the synaptic efficacy is a piece-wise continuous function of time with steps whenever a spike occurs. The amplitude of each step depends on the relative timing of previous spikes.

2.1 Instantaneous weight changes

Let us first concentrate on the effect of presynaptic spikes. Each spike that arrives at the presynaptic terminal can trigger a change in the synaptic efficacy even without additional postsynaptic action potentials (Alonso et al. 1990; Nelson et al. 1993; Urban and Barrionuevo 1996; Salin et al. 1996). In the case of so-called (non-Hebbian) presynaptic LTP, the amplitude a_1^{pre} of these changes is positive; cf. Fig. 1A. In addition

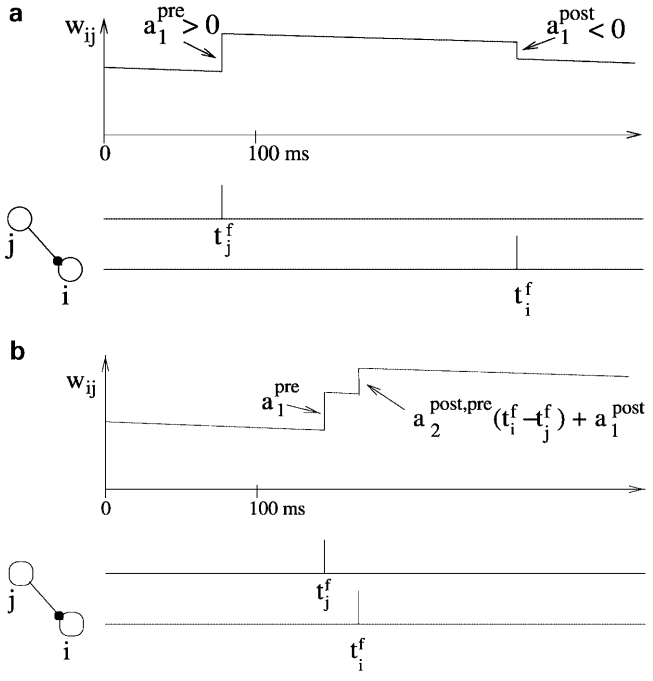

Fig. 1A,B. The lower part of each graph shows presynaptic spikes (neuron j) and postsynaptic spikes (neuron i). The upper part shows the evolution of the weight w_{ij}. **A**. A zero-order term $a_0 < 0$ can lead to a decrease of the synaptic weight w_{ij} even in the absence of any spike activity. Linear order terms cause sudden weight changes whenever a presynaptic spike arrives or a postsynaptic action potential is fired. For $a_1^{\text{pre}} > 0$, presynaptic spike arrival at time t_j^f leads to a positive weight change $\Delta w_{ij} = a_1^{\text{pre}}$. For $a_1^{\text{post}} < 0$, each postsynaptic spike decreases the synaptic efficacy. **B**. In case of Hebbian plasticity with $a_2^{\text{post,pre}}(t_i^f - t_j^f) > 0$, a postsynaptic spike t_i^f fired shortly after presynaptic spike arrival at t_j^f, gives rise to a weight change $a_2^{\text{post,pre}}(t_i^f - t_j^f) + a_1^{\text{post}}$ which can be positive, even if $a_1^{\text{post}} < 0$. (Gerstner and Kistler 2002b)

to this non-Hebbian effect there is also a contribution to the change that depends on the time lapsed since the last postsynaptic action potential(s). In analogy to the spike response formalism (Gerstner and van Hemmen 1992; Kistler et al. 1997) we use an integral kernel $a_2^{\text{pre,post}}$ to describe the amplitude of the change in the synaptic efficacy. Altogether we have

$$\frac{\mathrm{d}}{\mathrm{d}t} w_{ij}(t) = S_j(t) \left[a_1^{\text{pre}} + \int_0^\infty a_2^{\text{pre,post}}(s) S_i(t-s)\, \mathrm{d}s \right] \quad (1)$$

where $S_j(t) = \sum_f \delta(t - t_j^f)$ and $S_i(t) = \sum_f \delta(t - t_i^f)$ are pre- and postsynaptic spike trains, respectively, $\{t_i^f, f = 1, 2, \ldots\}$ the firing times of neuron i, and δ the Dirac delta function. The value of the kernel $a_2^{\text{pre,post}}(s)$ gives the weight change if a postsynaptic action potential is followed by presynaptic spike arrival with delay s. In pyramidal cells of the hippocampus, for example, this term is negative (Markram et al. 1997; Bi and Poo 1998).

Changes in the synaptic efficacy can also be triggered by postsynaptic action potentials. Similarly to presynaptically triggered changes, the amplitude of the weight change consists of at least two contributions: a non-Hebbian term a_1^{post} and the correlation term described by an integral kernel $a_2^{\text{post,pre}}$; cf. Fig. 1B. Together with an activity-independent term a_0 the total change in the synaptic efficacy reads

$$\begin{aligned} \frac{\mathrm{d}}{\mathrm{d}t} w_{ij}(t) = a_0 \\ + S_j(t) \left[a_1^{\text{pre}} + \int_0^\infty a_2^{\text{pre,post}}(s) S_i(t-s)\, \mathrm{d}s \right] \\ + S_i(t) \left[a_1^{\text{post}} + \int_0^\infty a_2^{\text{post,pre}}(s) S_j(t-s)\, \mathrm{d}s \right], \quad (2) \end{aligned}$$

cf. Kistler and van Hemmen (2000). Note that all parameters a_0, a_1^{pre}, a_1^{post} and all kernels $a_2^{\text{pre,post}}$, $a_2^{\text{post,pre}}$ may also depend upon the actual value of the synaptic efficacy. A possible consequence of this dependence, for example, is that it becomes increasingly difficult to strengthen a synapse that has already been potentiated and, vice versa, to weaken a depressed synapse (Ngezahayo et al. 2000).

Equation 2 can easily be extended so as to include more complex dependencies between pre- and postsynaptic spikes or between different consecutive pre- or postsynaptic spikes. We can include higher-order terms such as $S_j(t) \int_0^\infty a_2^{\text{pre,pre}}(s) S_j(t-s) ds$ and $S_i(t) \int_0^\infty a_2^{\text{post,post}}(s) S_i(t-s) \mathrm{d}s$ that are quadratic in pre- or postsynaptic spike trains. Nevertheless, the essence of Hebbian synaptic plasticity is captured by the terms that are *bilinear* in the pre- and postsynaptic spike train. The kernel $a_2^{\text{post,pre}}(s)$, which is usually positive, gives the amount of the weight change when a presynaptic spike is followed by a postsynaptic action potential with delay s; cf. the left half of the graph shown in Fig. 2A. The kernel $a_2^{\text{pre,post}}(s)$ describes the right half of the graph, i.e., the amount of change if the timing is the other way around. Since experimental results on STDP are usually

presented in graphical form such as in Fig. 2A, we define a 'learning window' W as

$$W(s) = \begin{cases} a_2^{\text{post,pre}}(-s), & s < 0, \\ a_2^{\text{pre,post}}(s), & s > 0 \ , \end{cases} \tag{3}$$

where $s = t_j^f - t_i^f$ is the delay between presynaptic spike arrival and postsynaptic firing. The change of the synaptic weight can thus be written as

$$\begin{aligned} \frac{\mathrm{d}}{\mathrm{d}t} w_{ij}(t) = a_0 + a_1^{\text{pre}} S_j(t) + a_1^{\text{post}} S_i(t) \\ + S_j(t) \int_0^\infty W(s) S_i(t-s) \mathrm{d}s \\ + S_i(t) \int_0^\infty W(-s) S_j(t-s) \mathrm{d}s \ . \end{aligned} \tag{4}$$

Note that a negative argument of the learning window W refers to presynaptic spike arrival *before* postsynaptic firing.

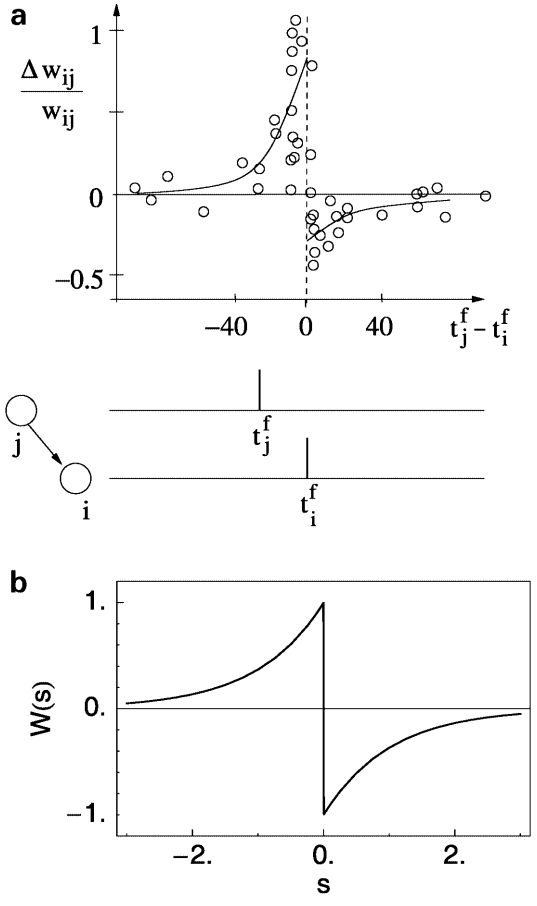

Fig. 2A. Timing requirements between pre- and postsynaptic spikes. Experimentally measured weight changes (circles) as a function of $t_j^f - t_i^f$ in milliseconds overlayed on a schematic two-phase learning window (solid line). Synapses are strengthened (LTP) if the presynaptic spike *precedes* the postsynaptic one; if the timing is the other way around, synaptic weights are decreased. Data points redrawn after the experiments of (Bi and Poo 1998). **B**. Asymmetric exponential learning window W as a function of the time difference s between presynaptic spike arrival and postsynaptic firing with $A_+ = -A_- = 1$ and $\tau_\pm = \tau = 1$ (arbitrary units); cf. Eq. (5). (Gerstner and Kistler 2002b)

A simple choice for the learning window – and thus for the kernels $a_2^{\text{post,pre}}$ and $a_2^{\text{pre,post}}$ – inspired by experimental findings is

$$W(s) = \begin{cases} A_+ \exp[s/\tau_+] & \text{for } s < 0 \ , \\ A_- \exp[-s/\tau_-] & \text{for } s > 0 \ , \end{cases} \tag{5}$$

with constants $A_\pm$ and $\tau_\pm$. If $A_+ > 0$ and $A_- < 0$ then the synaptic efficacy is increased if presynaptic spikes arrive slightly *before* the postsynaptic firing ($W(s) > 0$ for $s < 0$) and the synapse is weakened if presynaptic spikes arrive a few milliseconds *after* the output spike ($W(s) < 0$ for $s > 0$); cf. Fig. 2B. This choice of parameters gives raise to Hebbian learning because the presynaptic spike "has taken part in firing the neuron" (Hebb 1949) and the synapse is strengthened. A different choice, i.e., $A_+ < 0$ and $A_- > 0$, leads to the opposite type of behavior which is thus termed 'anti-Hebbian plasticity'.

2.2 Bounds for the synaptic weights

In order to obtain a realistic description of synaptic plasticity we have to make sure that the synaptic efficacy stays within certain bounds. Excitatory synapses, for example, should have a positive weight and must not exceed a maximum value of, say, $w_{ij} = 1$. We can implement these constraints in Eq. (5) by setting $A_- = w_{ij} a_-$ and $A_+ = (1 - w_{ij}) a_+$. The remaining terms in Eq. (2) can be treated analogously[1]. For each positive term (leading to a weight increase) we assume a weight dependence $\propto (1 - w_{ij})$, while for each negative term (leading to a weight decrease) we assume a weight dependence $\propto w_{ij}$ ('soft bounds'). It thus becomes increasingly difficult to strengthen (or weaken) a synapse that approaches its upper (or lower) bound (Kistler and van Hemmen 2000).

Another way to restrict the synaptic efficacy to a finite interval is to simply discard weight changes that violate the boundary condition ('hard bounds'). As soon as the synaptic efficacy has reached its upper (or lower) bound it is no longer potentiated (or depressed). Both hard and soft bounds can be seen as special cases of the learning equation 2 with weight-dependent parameters and kernels where terms leading to potentiation are proportional to $(1 - w_{ij})^{1/p}$ and all terms leading to depression are proportional to $(w_{ij})^{1/p}$. Here, p is a positive constant that describes the 'hardness' of the boundary condition. With $p = 1$ we recover soft bounds whereas $p \to \infty$ yields hard bounds; cf. Fig. 3.

The stationary weight distribution for a given type of stimulation can depend critically on how synaptic

[1] Note that w_{ij} is a step function of time with discontinuities whenever a presynaptic spike arrives or a postsynaptic action potential is triggered. In order to obtain a well-defined differential equation we specify that the amplitude of the step depends on the value of w_{ij} immediately *before* the spike. In mathematical terms, we impose the condition that $w_{ij}(t)$ is continuous from left, i.e., that $\lim_{s \to 0, s > 0} w_{ij}(t - s) = w_{ij}(t)$.

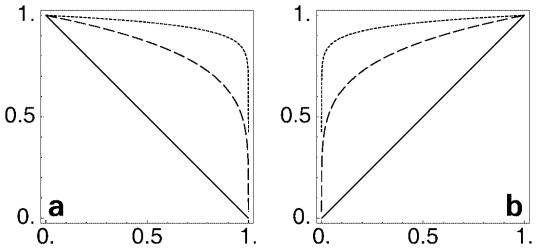

Fig. 3A,B. Implementation of synaptic bounds. **A**. Terms leading to potentiation are proportional to $(1-w_{ij})^{1/p}$ so that it becomes increasingly difficult to strengthen a synapse that approaches its upper bound $w_{ij}=1$. The parameter p describes the character of the boundary condition: $p=1$ (solid line), $p=5$ (dashed line), $p=20$ (dotted line). **B**. Terms leading to depression are proportional to $(w_{ij})^{1/p}$ (similar plot as in A)

bounds are implemented (van Rossum et al. 2000). For soft bounds (small p) the synapses 'feel' the restriction even if they are far from their boundary. Stationary weights are reached as soon as potentiation and depression balance each other at some intermediate values of the synaptic efficacy. For hard bounds (large p) the synaptic efficacies can evolve freely unless they approach the extreme values. The final distribution is thus characterized by a state where almost all synapses are saturated at either of their boundary values. This observation will be illustrated in a concrete example in Sect. 5.

2.3 Extensions

Several types of neurons can fire two different forms of action potentials depending on how they are stimulated. Synaptic weight changes do not only depend on pre- and postsynaptic firing times but also on the type of postsynaptic action potential. Cerebellar Purkinje cells, for example, receive input from two different fiber systems, viz., the massive input from about 200,000 parallel fibers and the exceptionally strong input from one additional climbing fiber (Ito 1984). A single climbing fiber spike suffices to trigger a postsynaptic action potential followed by a short burst of spikelets, the so-called *complex spike*. Parallel fiber activation, on the other hand, triggers regular sodium spikes (*simple spikes*).

Hippocampal pyramidal cells and cerebellar Purkinje cells are the two standard systems for the investigation of synaptic plasticity. Whereas hippocampal pyramidal cells are usually studied in the context of long-term potentiation (LTP), parallel fiber-Purkinje cell synapses have most extensively been studied because of their ability to undergo activity-induced long-term depression (LTD) (Ito and Kano 1982). In pyramidal cells, back-propagating action potentials that remove the magnesium block of NMDA receptors so as to allow extracellular calcium ions to enter the cell are thought to play a major role in the induction of LTP (Bliss and Collingridge 1993; Linden 1999). Cerebellar Purkinje cells, however, are devoid of NMDA receptors. Nevertheless, dendritic calcium signals generated by voltage-activated calcium channels during complex spikes are necessary for the induction of cerebellar LTD (Konnerth and Eilers 1994; Denk et al. 1995; Daniel et al. 1998; Lev-Ram et al. 1997). Plasticity at parallel fiber-Purkinje cell synapses is thus not determined by the joint activity of pre- and postsynaptic cells but rather by the joint activation of two distinct *presynaptic* fibers, namely parallel and climbing fibers (Ito and Kano 1982; Karachot et al. 1994).

There is increasing evidence that the induction of cerebellar LTD depends on the relative timing of climbing- and parallel fiber spikes similar to the timing requirements for pre- and postsynaptic spikes in pyramidal cells. Whether climbing- or parallel fiber spikes have to be first in order to induce LTD, however, is still a matter of fervent debate (Hirano 1991; Karachot et al. 1994; Schreurs et al. 1996; Schreurs et al. 1997; Lev-Ram et al. 1997; Wang et al. 2000). In any case, the above formalism can easily be extended so as to describe synaptic plasticity that is driven by correlations in parallel- and climbing fiber spike trains. A straightforward generalization of Eq. (4) yields

$$\begin{aligned}\frac{\mathrm{d}}{\mathrm{d}t}w_{ij}(t) = a_0 + a_1^{\mathrm{pre}}S_j(t) + a_1^{\mathrm{post}}S_i(t) + a_1^{\mathrm{cf}}S_i^{\mathrm{cf}}(t)\\ + S_j(t)\int_0^\infty W(s)S_i(t-s)\mathrm{d}s\\ + S_i(t)\int_0^\infty W(-s)S_j(t-s)\mathrm{d}s\\ + S_j(t)\int_0^\infty W_{\mathrm{cf}}(s)S_i^{\mathrm{cf}}(t-s)\mathrm{d}s\\ + S_i^{\mathrm{cf}}(t)\int_0^\infty W_{\mathrm{cf}}(-s)S_j(t-s)\mathrm{d}s\ .\end{aligned} \tag{6}$$

Here, w_{ij} is the strength of the synapse of parallel fiber j to Purkinje cell i, S_j and S_i are the pre- and postsynaptic spike trains, respectively, and S_i^{cf} is the corresponding climbing fiber spike train. Finally, W_{cf} is the learning window that describes synaptic weight changes due to correlations in parallel- and climbing fiber spike trains (Kistler and van Hemmen 1999; Kistler et al. 2000).

3 Weight dynamics

In this section we want to relate the synaptic weight change to the statistical properties of the input. In order to keep our results general we do not specify a particular neuron model and consider the set of presynaptic spike arrival times $(t_j^1, t_j^2, \ldots)$ as a random variable. The underlying 'randomness' may have several reasons. For example, different stimulation paradigms ('input patterns') may be selected one by one by the experimenter. Moreover, we do not want to restrict ourselves to deterministic neuron models. Hence, the randomness can also be produced by a stochastic neuron model that is used in order to account for noise. In this case, the output spike train can be a random variable even if the

input spike trains are fixed. A simple example is a Poisson neuron model that generates output spikes via an inhomogeneous Poisson process with an intensity that is a function of the membrane potential. In any case, we consider the set of spike trains $(S_1, \ldots, S_i, S_j, \ldots, S_N)$, i.e., pre- *and* postsynaptic trains, to be drawn from a stochastic ensemble. The specific properties of the chosen neuron model are thus implicitly described by the association of pre- and postsynaptic trains within the ensemble. Note that this formalism includes deterministic models as a special case if the ensemble contains only a single postsynaptic spike train for any given set of presynaptic spike trains. In the following discussion, all averages denoted by $\langle\cdot\rangle_E$ are to be taken relative to this ensemble.

For the time being we are interested only in the long-term behavior of the synaptic weights and not in the fluctuations that are caused by individual spikes. We therefore calculate the expectation value of the weight change over a certain interval of time,

$$\big\langle w_{ij}(t+T) - w_{ij}(t)\big\rangle_E = \left\langle \int_t^{t+T} \frac{\mathrm{d}}{\mathrm{d}t} w_{ij}(t')\mathrm{d}t' \right\rangle_E . \tag{7}$$

With the abbreviation

$$\langle f(t)\rangle_T \equiv T^{-1}\int_t^{t+T} f(t')\mathrm{d}t' \tag{8}$$

we obtain from Eq. (4)

$$\begin{aligned}\frac{\big\langle w_{ij}(t+T) - w_{ij}(t)\big\rangle_E}{T} &= a_0 + a_1^{\mathrm{pre}}\big\langle\big\langle S_j(t)\big\rangle_T\big\rangle_E + a_1^{\mathrm{post}}\big\langle\big\langle S_i(t)\big\rangle_T\big\rangle_E \\ &\quad + \int_0^\infty W(s)\big\langle\big\langle S_i(t-s)S_j(t)\big\rangle_T\big\rangle_E \,\mathrm{d}s \\ &\quad + \int_{-\infty}^0 W(s)\big\langle\big\langle S_i(t)S_j(t+s)\big\rangle_T\big\rangle_E \,\mathrm{d}s \ . \end{aligned} \tag{9}$$

If the time interval T is long compared to typical interspike intervals then the time average is taken over many pre- or postsynaptic spikes. We can thus assume that the average $\big\langle\big\langle S_i(t)S_j(t+s)\big\rangle_T\big\rangle_E$ does not change if we replace t by $t-s$ as long as $s \ll T$. Furthermore, if $W(s)$ decays to zero sufficiently fast as $|s| \to \infty$ then the integration over s in the last term of Eq. (9) can be restricted to a finite interval determined by the width of the learning window W . In this case it is safe to replace $\big\langle\big\langle S_i(t)S_j(t+s)\big\rangle_T\big\rangle_E$ by $\big\langle\big\langle S_i(t-s)S_j(t)\big\rangle_T\big\rangle_E$ and to collect the last two terms of Eq. (9) into a single integral, provided that the width of the learning window is small as compared to T. With this approximation we find

$$\begin{aligned}\frac{\big\langle w_{ij}(t+T) - w_{ij}(t)\big\rangle_E}{T} &= a_0 + a_1^{\mathrm{pre}}\big\langle\big\langle S_j(t)\big\rangle_T\big\rangle_E + a_1^{\mathrm{post}}\big\langle\big\langle S_i(t)\big\rangle_T\big\rangle_E \\ &\quad + \int_{-\infty}^\infty W(s)\big\langle\big\langle S_i(t-s)S_j(t)\big\rangle_T\big\rangle_E \,\mathrm{d}s \ . \end{aligned} \tag{10}$$

The instantaneous firing rate $\nu_i(t)$ of neuron i is the ensemble average of its spike train,

$$\nu_i(t) \equiv \big\langle S_i(t)\big\rangle_E \ . \tag{11}$$

Similarly, we define the joint firing rate ν_{ij} of neuron i and j as

$$\nu_{ij}(t,t') \equiv \big\langle S_i(t)S_j(t')\big\rangle_E \ , \tag{12}$$

which is the joint probability density to find both a spike at time t and at time t' in neuron i and j, respectively. Note that $\nu_{ij}(t,t')$ is a probability density both in t and t' and thus has units of one over time squared.

Since averaging is a linear operation we can exchange ensemble average and time average. We obtain the following expression for the expected weight change in the interval from t to $t+T$ as a function of the statistical properties of the spike trains,

$$\begin{aligned}\frac{\big\langle w_{ij}(t+T) - w_{ij}(t)\big\rangle_E}{T} &= a_0 + a_1^{\mathrm{pre}}\big\langle\nu_j(t)\big\rangle_T + a_1^{\mathrm{post}}\big\langle\nu_i(t)\big\rangle_T \\ &\quad + \int_{-\infty}^\infty W(s)\big\langle\nu_{ij}(t-s,t)\big\rangle_T \mathrm{d}s \ . \end{aligned} \tag{13}$$

The time average $\langle\nu_{ij}(t-s,t)\rangle_T$ is the correlation function of pre- and postsynaptic spike trains on the interval $[t, t+T]$. This function clearly depends on the chosen neuron model and, in particular, on the actual value of the weight vector. In deriving Eq. (13) we have already had to assume that the correlations are a slowly varying function of time. For the sake of consistency we thus have the requirement that the weight vector itself is a slowly varying function of time. If this is the case then we can exploit the self-averaging property of the weight vector and argue that fluctuations around the expectation value are negligible so that Eq. (13) is a good approximation of the actual value of the weight vector. We thus drop the ensemble average on the left-hand side of Eq. (13) and find for the time-averaged change of the synaptic weight the following learning equation,

$$\begin{aligned}\frac{\mathrm{d}}{\mathrm{d}t}\big\langle w_{ij}(t)\big\rangle_T &= a_0 + a_1^{\mathrm{pre}}\big\langle\nu_j(t)\big\rangle_T \\ &\quad + a_1^{\mathrm{post}}\big\langle\nu_i(t)\big\rangle_T \\ &\quad + \int_{-\infty}^\infty W(s)\big\langle\nu_{ij}(t-s,t)\big\rangle_T \mathrm{d}s \ ; \end{aligned} \tag{14}$$

cf. (Kempter et al. 1999). As expected, the long-term dynamics of the synaptic weights depends on the correlation of pre- and postsynaptic spike trains at the time scale of the learning window.

The joint probability density $\nu_{ij}(t,t') = \langle S_i(t)S_j(t')\rangle_E$ to find an input spike at synapse j at time t' and an output spike of neuron i at time t equals, according to Bayes' Theorem, the probability of observing an input spike at time t' times the conditional probability of observing an output spike at time t given the input spike at time t', i.e.,

$$v_{ij}(t,t') = \langle S_i(t)|\text{input spike at } t'\rangle_E \langle S_j(t')\rangle_E \ . \quad (15)$$

For $w_{ij} = 0$ pre- and postsynaptic firing times are independent so that $v_{ij}(t,t') = \langle S_i(t)\rangle_E \langle S_j(t')\rangle_E$. Neurons usually receive synaptic input from a large number of presynaptic neurons. Hence, the effect of a *single* presynaptic spike on the firing of a postsynaptic action potential is small so that we can expand $v_{ij}(t,t')$ about $w_{ij} = 0$,

$$\begin{aligned} v_{ij}(t,t') &= \langle S_i(t)\rangle_E \langle S_j(t')\rangle_E \\ &\quad + w_{ij}\, c_{\mathrm{SS}}(t-t')\Theta(t-t')\langle S_j(t')\rangle_E \\ &\quad + \mathrm{O}\left(w_{ij}^2\right) \ . \end{aligned} \quad (16)$$

Here, $c_{\mathrm{SS}}(t-t')$ describes the spike-spike correlations as a function of the time interval between presynaptic spike arrival and postsynaptic firing. Causality is accounted for by the Heaviside function, $\Theta(t-t')$, expressing the fact that a presynaptic spike cannot have any effect on postsynaptic spikes that have been fired before. The first term on the right-hand side is thus the 'chance level' to find two spikes at t and t', respectively, if the neurons were firing independently at rates $\nu_i(t) = \langle S_i(t)\rangle_E$ and $\nu_j(t') = \langle S_j(t')\rangle_E$. The remaining terms describe correlations that are due to synaptic coupling.

If we substitute Eq. (16) into Eq. (14) and keep only first order terms in w_{ij} we find

$$\begin{aligned} \frac{\mathrm{d}}{\mathrm{d}t}\langle w_{ij}(t)\rangle_T &= a_0 + a_1^{\mathrm{pre}}\langle \nu_j(t)\rangle_T + a_1^{\mathrm{post}}\langle \nu_i(t)\rangle_T \\ &\quad + \int_{-\infty}^{\infty} W(s)\langle \nu_i(t-s)\nu_j(t)\rangle_T \mathrm{d}s \\ &\quad + \langle w_{ij}(t)\rangle_T \langle \nu_j(t)\rangle_T W_- \ , \end{aligned} \quad (17)$$

with $W_- = \int_0^\infty W(-s)c_{\mathrm{SS}}(s)\mathrm{d}s$. The correlation between pre- and postsynaptic activity that drives synaptic weight changes consists of two contributions. The integral over the learning window in Eq. (17) describes correlations in the instantaneous firing rate. The last term on the right-hand side of Eq. (17) finally accounts for spike-spike correlations of pre- and postsynaptic neurons.

4 Learning to be precise

As a concrete example for STDP-induced weight dynamics we discuss a phenomenon that may be important in networks based on a time-coding paradigm, i.e., in networks where information is coded in the precise firing time of individual action potentials. We show that an asymmetric learning window can selectively strengthen synapses that deliver precisely timed spikes at the expense of others that deliver spikes with a broad temporal jitter. This is obviously a way to reduce the noise level of the membrane potential and to increase the temporal precision of the postsynaptic response (Kistler and van Hemmen 2000).

4.1 The model

We consider a neuron i that receives spike input from N presynaptic neurons via synapses with weights w_{ij}, $1 \le j \le N$. The membrane potential $u_i(t)$ is described by the spike response formalism with response kernels ϵ ('postsynaptic potential') and η ('afterpotential'), and the last postsynaptic firing time $\hat{t}_i$, i.e.,

$$\begin{aligned} u_i(t) &= \eta(t-\hat{t}_i) + \\ &\quad N^{-1}\sum_{\substack{j=1 \\ (j\neq i)}}^{N} \int_0^\infty w_{ij}(t-s)\epsilon(s)S_j(t-s)\mathrm{d}s \ ; \end{aligned} \quad (18)$$

cf. (Gerstner and van Hemmen 1992; Kistler et al. 1997). The ϵ kernel describes the shape of a postsynaptic potential. In the following, we adopt a simple alpha function,

$$\epsilon(s) = s/\tau_{\mathrm{M}} \exp(1 - s/\tau_{\mathrm{M}})\Theta(s) \ , \quad (19)$$

with τ_{M} as the membrane time constant and Θ as the Heaviside function with $\Theta(s) = 1$ if $s > 0$ otherwise $\Theta(s) = 0$. For the sake of simplicity we set $\tau_{\mathrm{M}} = 1$, i.e., we give all times in units of the membrane time constant.

In order to account for noise we adopt a stochastic spike triggering criterion. Postsynaptic spikes are fired at a rate ν that is a nonlinear function of the membrane potential,

$$\nu(u) = \nu_{\max}\Theta(u - \vartheta) \ . \quad (20)$$

If the membrane potential is below the firing threshold ϑ, the neuron is quiescent. If the membrane potential reaches the threshold, the neuron will respond with an action potential within the characteristic response time $\nu_{\max}^{-1}$. We refer to this neuron model as the *nonlinear Poisson model*. Note that the output rate is determined by the shape of the η kernel rather than by $\nu(u)$. In particular, the constant $\nu_{\max}$ is not the maximum firing rate but the reliability of the neuron. The larger $\nu_{\max}$, the faster the neuron will fire after the threshold has been reached. For $\nu_{\max} \to \infty$ we recover the sharp firing threshold of a noiseless neuron model.

Presynaptic spike trains are described by inhomogeneous Poisson processes with a time-dependent firing intensity $\nu_i(t)$. More specifically, we consider a volley of spikes that reaches the postsynaptic neuron approximately at time t_0. The width of the volley is determined by the time course of the firing intensities ν_i. For the sake of simplicity we use bell-shaped intensities with a width σ_i centered around t_0. The width σ_i is a measure for the temporal precision of the spikes that are conveyed via synapse i. The intensities are normalized so that, on average, each presynaptic neuron contributes a single action potential to the volley.

Synaptic plasticity is implemented along the lines of Sect. 2. Synaptic weights change whenever presynaptic

spikes arrive or when postsynaptic action potentials are triggered,

$$\frac{\mathrm{d}}{\mathrm{d}t}w_{ij}(t) = a_0 + a_1^{\mathrm{pre}} S_j(t) + a_1^{\mathrm{post}} S_i(t) + S_j(t)\int_0^\infty W(s) S_i(t-s)\mathrm{d}s + S_i(t)\int_0^\infty W(-s) S_j(t-s)\mathrm{d}s \ ; \qquad (21)$$

cf. Eqs. 2–3. In order to describe Hebbian plasticity we choose an asymmetric exponential learning window W that is positive for $s < 0$ and negative for $s > 0$,

$$W(s) = \begin{cases} A_+ \exp(s/\tau), & if\ s < 0 \\ A_- \exp(-s/\tau), & if\ s > 0 \end{cases} \qquad (22)$$

with $A_+ > 0$ and $A_- < 0$; cf. Fig. 2.

In addition to the Hebbian term, we also take advantage of the non-Hebbian terms a_1^{pre} and a_1^{post} in order to ensure that the postsynaptic firing rate stays within certain bounds. More precisely, we use $0 < a_1^{\mathrm{pre}} \ll 1$ and $-1 \ll a_1^{\mathrm{post}} < 0$. A positive value for a_1^{pre} leads to growing synapses even if only the presynaptic neuron is active. This effect will bring the neuron back to threshold even if all synaptic weights were strongly depressed. A small negative value for a_1^{post}, on the other hand, leads to a depression of the synapse, if the postsynaptic neuron is firing at an excessively high rate. Altogether, the non-Hebbian terms keep the neuron at its operating point.

Apart from the postsynaptic firing rate we also want individual synaptic weights restricted to a finite interval. We thus introduce a dependence of the parameters in Eqs. 21 and 22 on the actual value of the synaptic weight as described in Sect. 2. All terms leading to potentiation are proportional to $(1 - w_{ij})^{1/p}$ and all terms leading to depression to $(w_{ij})^{1/p}$. The parameter $p > 0$ describes the 'hardness' of the bounds. Altogether we have

$$\frac{\mathrm{d}}{\mathrm{d}t}w_{ij}(t) = a_1^{\mathrm{pre}}[1 - w_{ij}(t)]^{1/p} S_j(t) + a_1^{\mathrm{post}}[w_{ij}(t)]^{1/p} S_i(t) + S_j(t)\int_0^\infty W(s) S_i(t-s)\mathrm{d}s + S_i(t)\int_0^\infty W(-s) S_j(t-s)\mathrm{d}s \ , \qquad (23)$$

and $A_+ = a_+[1 - w_{ij}(t)]^{1/p}$, $A_- = a_-[w_{ij}(t)]^{1/p}$ with constants $a_+ > 0$ and $a_- < 0$. The constant term a_0 describing weight decay has been discarded.

4.2 Firing time distribution

We have seen in Sect. 3 that the evolution of synaptic weights depends on correlations of pre- and postsynaptic spike trains at the time scale of the learning window. In order to calculate this correlation we need the joint probability density for pre- and postsynaptic spikes ('joint firing rate'), $\nu_{ij}(t, t')$; cf. Eq. (16). Here, we are interested in neurons that receive synaptic input from many presynaptic cells. The effect of a single presynaptic spike on the firing time of the postsynaptic neuron can thus be neglected. In this case, the joint firing rate is just the product of pre- and postsynaptic firing intensities,

$$\nu_{ij}(t, t') \approx \nu_i(t)\nu_j(t') \ . \qquad (24)$$

It thus remains to determine the postsynaptic firing time distribution given the presynaptic spike statistics. The output spike train is the result of a doubly stochastic process (Cox 1955; Bartlett 1963) in the sense that first presynaptic spike trains are produced by inhomogeneous Poisson processes so that the membrane potential is in itself a stochastic process. In a second step the output spike train is generated from a firing intensity that is a function of the membrane potential. Though the composite process is not equivalent to an inhomogeneous Poisson process, the output spike train can be approximated by such a process with an intensity that is given by the expectation of the rate ν with respect to the input statistics (Kistler and van Hemmen 2000),

$$\bar{\nu}_i(t) = \langle \nu[u_i(t)] \rangle \ . \qquad (25)$$

The angular brackets denote an average over the ensemble of input spike trains.

Due to refractoriness, the neuron cannot fire two spikes directly one after the other; an effect that is clearly not accounted for by a description in terms of a firing intensity as in Eq. (25). A possible way out is to assume that the afterpotential is so strong that the neuron can fire only a single spike followed by a long period of silence. In this case we can focus on the probability density $p_i^{\mathrm{first}}(t)$ of the *first* postsynaptic spike which is given by the probability density to find a spike at t times the probability that there was no spike before, i.e.,

$$p_i^{\mathrm{first}}(t) = \bar{\nu}_i(t) \exp\left[-\int_{\hat{t}}^{t} \bar{\nu}_i(t')\mathrm{d}t'\right] \ . \qquad (26)$$

The lower bound $\hat{t}$ is the time when the neuron has fired its last spike from then on we consider the next spike to be the 'first' one.

Given the statistics of the presynaptic volley of action potentials we are now able to calculate the expected firing intensity $\bar{\nu}_i(t)$ of the postsynaptic neuron and hence the firing time distribution $p_i^{\mathrm{first}}(t)$ of the first action potential that will be triggered by the presynaptic volley. In certain limiting cases, explicit expressions for $p_i^{\mathrm{first}}(t)$ can be derived; cf. Fig. 4. See Kistler and van Hemmen (2000) for details.

4.3 Stationary synaptic weights

In the limiting case of many presynaptic neurons and strong refractoriness, the joint firing rate of pre- and postsynaptic neurons is given by

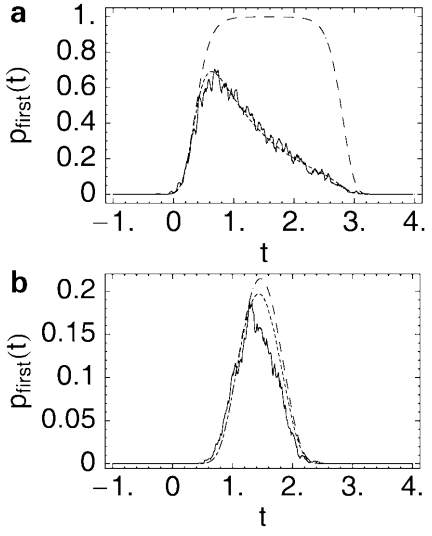

Fig. 4A,B. Probability density of the postsynaptic firing time with (p_{first}, dotted line) and without refractoriness ($\bar{\nu}$, dashed line). The solid line shows a simulation of a neuron that receives input from $N = 100$ presynaptic neurons via synapses with strength $w_{ij} = 1/N$. Presynaptic spike trains are generated by an inhomogeneous Poisson process with rate function $\nu_j = (2\pi\sigma^2)^{-1/2} \exp\left[-t^2/2\sigma^2\right]$ and $\sigma = 1$. The ϵ kernel is an alpha function, $t\exp(1-t)$, so that the maximum of the membrane potential amounts to $u = 1$, if all spikes were to arrive simultaneously. The postsynaptic response is characterized by $\nu_{\max} = 1$ and $\vartheta = 0.5$ in **A** and $\vartheta = 0.75$ in **B**. Increasing the threshold improves the temporal precision of the postsynaptic response, but the overall probability of a postsynaptic spike is decreased. (Kistler and van Hemmen 2000)

$$v_{ij}(t,t') = p_i^{\text{first}}(t) v_j(t') \ . \tag{27}$$

We can use this result in Eq. (14) to calculate the change of the synaptic weight that is induced by the volley of presynaptic spikes and the postsynaptic action potential that may have been triggered by this volley. To this end we choose the length of the time interval T such that the time averages in learning equation 14 include all spikes within the volley and the postsynaptically triggered action potential.

A given combination of pre- and postsynaptic firing times will result in, say, a potentiation of the synaptic efficacy and the synaptic weight will be increased whenever this particular stimulus is applied. However, due to the soft bounds that we have imposed on the weight dynamics, the potentiating terms become less and less effective as the synaptic weight approaches its upper bound at $w_{ij} = 1$, because all terms leading to potentiation are proportional to $(1 - w_{ij})^{1/p}$. On the other hand, terms that lead to depression become increasingly effective due to their proportionality to $(w_{ij})^{1/p}$. At some point potentiation and depression balance each other so that a fixed point for the (time-averaged) synaptic weight is reached. The fixed point equation can be derived from Eq. (14),

$$\begin{aligned} \frac{\mathrm{d}}{\mathrm{d}t}\left\langle w_{ij}(t)\right\rangle_T = 0 \Leftrightarrow [1 - \left\langle w_{ij}(t)\right\rangle_T]^{1/p} \Delta_{\text{LTP}} \\ = -[\left\langle w_{ij}(t)\right\rangle_T]^{1/p} \Delta_{\text{LTD}} \end{aligned} \tag{28}$$

with

$$\begin{aligned} \Delta_{\text{LTP}} = a_1^{\text{pre}} \left\langle v_j(t)\right\rangle_T \\ + a_+ \int_0^\infty \exp(-s/\tau) \left\langle p_i^{\text{first}}(t) v_j(t-s)\right\rangle_T \mathrm{d}s \end{aligned} \tag{29}$$

and

$$\begin{aligned} \Delta_{\text{LTD}} = a_1^{\text{post}} \left\langle p_i^{\text{first}}(t)\right\rangle_T \\ + a_- \int_0^\infty \exp(-s/\tau) \left\langle p_i^{\text{first}}(t-s) v_j(t)\right\rangle_T \mathrm{d}s \ , \end{aligned} \tag{30}$$

and easily be solved for $\left\langle w_{ij}(t)\right\rangle_T$.

Figure 5 shows the stationary synaptic weight as a function of the firing time statistics given in terms of the temporal jitter σ of pre- and postsynaptic spikes and their relative firing time. For small values of σ, that is, for precisely timed spikes, we recover the shape of the learning window. The synaptic weight saturates close to its maximum value if the presynaptic spikes arrive before the postsynaptic neuron is firing. If the timing is the other way around, the weight will be approximately zero. For increasing levels of noise in the firing times this relation is smeared out and the weight takes an intermediate value that is determined by non-Hebbian terms rather than by the learning window.

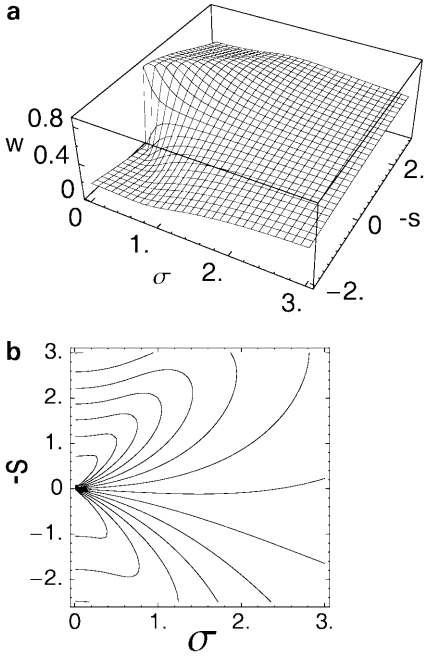

Fig. 5A,B. Stationary synaptic weights. **A**, 3D-plot of the stationary synaptic weight as a function of σ and s, where $\sigma^2 = \sigma_{\text{pre}}^2 + \sigma_{\text{post}}^2$ is the sum of the variances of pre- and postsynaptic firing time, and s is the mean time difference between the arrival of the presynaptic spike and the firing of the postsynaptic action potential. Note that the s-axis has been inverted for the sake of a better visibility of the graph. **B**, contour plot of the same function as in A. The parameters used to describe synaptic plasticity are $a_1^{\text{post}} = -0.01$, $a_1^{\text{pre}} = 0.001$, $a_+ = -a_- = 0.1$, $\tau = 1$, and $p = 1$. (Kistler and van Hemmen 2000)

4.4 The role of the firing threshold

We have seen that the stationary value of the synaptic weight is a function of the statistical properties of pre- *and* postsynaptic spike trains. The synaptic weights, on the other hand, determine the distribution of postsynaptic firing times. If we are interested in the synaptic weights that are produced by given input statistics, then we have to solve a self-consistency problem which can be done numerically by using explicit expressions for the firing time distributions derived along the lines sketched above.

Figure 6 shows an example of a neuron that receives spike input from two groups of presynaptic neurons. The first group is firing synchronously with a rather high temporal precision of $\sigma = 0.1$. The second group is also firing synchronously but with a much broader jitter of $\sigma = 1$. (All times are in units of the membrane time constant.) The spikes from both groups together form the spike volley that impinges on the postsynaptic neuron and induces changes in the synaptic weights. After a couple of these volleys have hit the neuron the synaptic weights will finally settle at their fixed point. Figure 6A shows the resulting weights for synapses that deliver precisely timed spikes together with those of the poorly timed group as a function of the neuronal firing threshold.

It is apparent from Fig. 6A that there is a certain domain for the neuronal firing threshold ($\vartheta \approx 0.25$) where synapses that convey precisely timed spikes are substantially stronger than synapses that deliver spikes with a broad temporal jitter. The key to understanding this result is the normalization of the postsynaptic firing rate by non-Hebbian terms in the learning equation.

The maximum value of the membrane potential, if all presynaptic neurons deliver one precisely timed spike, is $u_{\max} = 1$. The axis for the firing threshold in Fig. 6 therefore extends from zero to one. Let us consider high firing thresholds first. For $\vartheta \approx 1$ the postsynaptic neuron will reach its firing threshold only if all presynaptic spikes arrive almost simultaneously, which is rather unlikely given the high temporal jitter in the second group. The probability that the postsynaptic neuron is firing an action potential therefore tends to zero as $\vartheta \to 1$; cf. Fig. 6C. Each time the volley fails to trigger the neuron, the weights are increased due to presynaptic potentiation described by $a_1^{\text{pre}} > 0$. Therefore, irrespective of their temporal precision all synapses will finally reach an efficacy that is close to the maximum value.

On the other hand, if the firing threshold is very low, then a few presynaptic spikes suffice to trigger the postsynaptic neuron. Since the neuron can fire only a single action potential as a response to a volley of presynaptic spikes, the neuron will be triggered by the earliest spikes. The early spikes, however, are mostly spikes from presynaptic neurons with a broad temporal jitter. The postsynaptic neuron has therefore already fired its action potential before the spikes from the precise neurons arrive. Synapses that deliver precisely timed spikes are hence depressed, whereas synapses that deliver early but poorly timed spikes are strengthened; cf. (Mehta et al. 2000).

For some intermediate values of the firing threshold, synapses that deliver precisely timed spikes are strengthened at the expense of the other group. If the

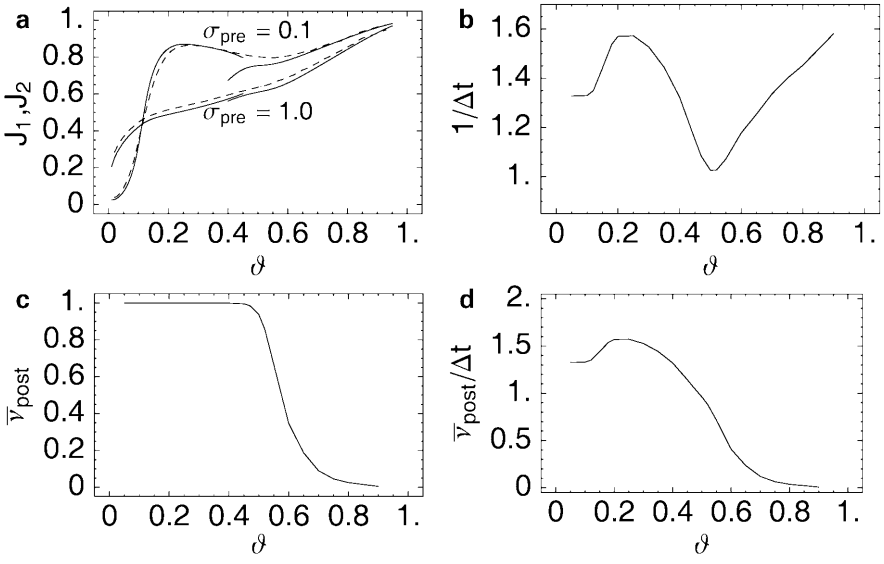

Fig. 6A. Synaptic weights for a neuron receiving input from two groups of synapses. One group ($n_1 = 20$) delivers precisely timed spikes ($\sigma_1 = 0.1$) and the other one ($n_2 = 80$) spikes with a broad distribution of arrival times ($\sigma_2 = 1.0$). The upper trace shows the resulting stationary synaptic weight for the group of precise synapses; the lower trace corresponds to the second group. The solid lines give the analytic result obtained for two limiting cases; see (Kistler and van Hemmen 2000) for details. The dashed lines show the results of a computer simulation. The parameters for the synaptic plasticity are the same as in Fig. 5. **B**, **C**, **D**, precision Δt^{-1}, reliability $\bar{\nu}_{\text{post}}$, and 'coding efficiency' $\bar{\nu}_{\text{post}}/\Delta t$ as a function of the threshold ϑ for the same neuron as in A. Reliability is defined as the overall firing probability $\bar{\nu}_{\text{post}} = \int \mathrm{d}t\, p_{\text{first}}(t)$. Precision is the inverse of the length of the interval containing 90 percent of the postsynaptic spikes, $\Delta t = t_2 - t_1$ with $\int_{-\infty}^{t_1} \mathrm{d}t\, p_{\text{first}}(t) = \int_{t_2}^{\infty} \mathrm{d}t\, p_{\text{first}}(t) = 0.05\bar{\nu}_{\text{post}}$. (Kistler and van Hemmen 2000)

firing threshold is just high enough so that a few early spikes from the poorly timed group are not able to trigger an action potential then the neuron will be fired most of the time by spikes from the precise group. These synapses are consistently strengthened due to the Hebbian learning rule. Spikes from the other group, however, are likely to arrive either much earlier or after the neuron has already fired so that the corresponding synapses are depressed.

A neuron that gets synaptic input predominantly from neurons that fire with a high temporal precision will also show little temporal jitter in its firing time relative to its presynaptic neurons. This is illustrated in Fig. 6B which gives the precision Δt of the postsynaptic firing time as a function of the firing threshold. The curve exhibits a clear peak for firing thresholds that favor 'precise' synapses. The precision of the postsynaptic firing time shows similarly high values in the high firing threshold regime. Here, however, the overall probability $\bar{\nu}_{\text{post}}$ for the neuron to reach the threshold is very low (Fig. 6C). In terms of a 'coding efficiency' defined by $\nu_{\text{post}}/\Delta t$ there is thus a distinct optimum for the firing threshold near $\vartheta = 0.25$ (Fig. 6D).

4.5 The role of synaptic bounds

Competition is an indispensable property of any system to exhibit phenomena like pattern formation. In the present case competition between synaptic weights is introduced indirectly by restricting the efficacy of individual synapses to a finite interval. A group of relatively strong synapses can control the postsynaptic firing time and, in doing so, can suppress synapses that deliver spikes at a later point in time. Presynaptic neurons are thus competing for their control of the postsynaptic firing time (Song et al. 2000). Without a restriction of synaptic efficacies to a finite interval, the absolute weight values would keep growing and, in general, no stationary distribution will be reached.

In the presence of synaptic bounds, a stationary weight distribution is reached as soon as net potentiation and net depression balance each other. This condition is expressed by the fixed point equation 28. Apart from the statistical properties of pre- and postsynaptic spike trains, the position of the fixed point $\bar{w}_{ij}$ depends also on how synaptic bounds are implemented, i.e., on the value of the parameter p. From Eq. (28) we find

$$\bar{w}_{ij} = \frac{(\Delta_{\text{LTP}})^p}{(\Delta_{\text{LTP}})^p - (\Delta_{\text{LTD}})^p} \left[1 + \left(\frac{-\Delta_{\text{LTD}}}{\Delta_{\text{LTP}}} \right)^p \right]^{-1} . \qquad (31)$$

The ratio $\Delta_{\text{LTD}}/\Delta_{\text{LTP}}$ of the strength of unbounded depression and potentiation thus controls the position of the fixed point and the value of the parameter p determines the sensitivity of the fixed point to this ratio cf. Fig. 7.

The role of the 'hardness' of the synaptic bounds is illustrated by the simulations shown in Fig. 8. Similar to the example in Fig. 6, a single neuron receives volleys of spikes from $N = 100$ presynaptic neurons. Each presy-

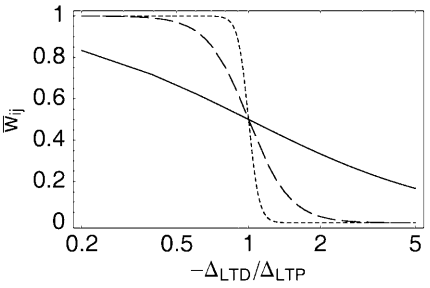

Fig. 7. Fixed point of the synaptic efficacy as a function of the ratio of potentiation and depression and various synaptic bounds ($p = 1$, solid line; $p = 5$, dashed line; $p = 20$, dotted line)

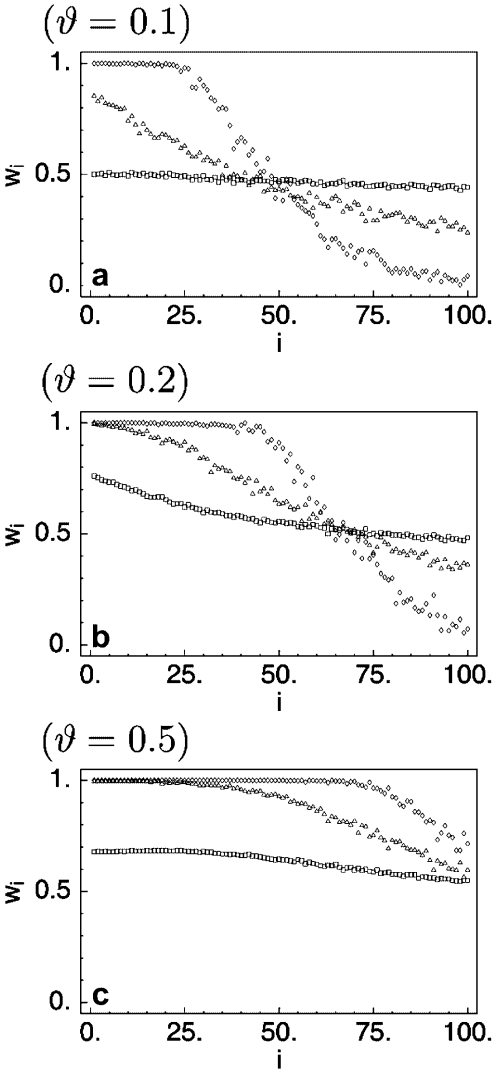

Fig. 8A–C. Distribution of stationary synaptic weights w_i for three different values of the firing threshold ϑ (**A**–**C**) and different synaptic bounds (symbols). The neuron receives synaptic input from $N = 100$ presynaptic neurons that deliver spikes with temporal precisions ranging from $\sigma_1 = 0.1$ to $\sigma_{100} = 1.0$. The abscissa gives the index of the presynaptic neurons sorted according to their precision; $i = 1$ corresponds to the neuron firing with the highest precision. The symbols correspond to different implementations of the synaptic bounds as characterized by the parameter p. Soft bounds ($p = 1$) result in stationary weights that are indicated by small squares. Increasingly 'hard' bounds are marked by triangles ($p = 5$) and diamonds ($p = 20$)

naptic neuron contributes (on average) a single spike to each volley. The width of the volleys is determined by the jitter in the presynaptic firing times. In contrast to Fig. 6, there are not only two different groups of neurons but each neuron has its own temporal precision σ_i, $i = 1 \ldots N$. The σ_i's are equidistantly distributed and range from $\sigma_1 = 0.1$ to $\sigma_N = 1.0$. Stimulating the postsynaptic neurons repeatedly with these volleys will finally lead to a stationary distribution of synaptic weights. For soft bounds ($p = 1$) the efficacy of synapses that convey precisely timed spikes is only slightly larger than the efficacy of synapses that deliver poorly timed spikes. The small difference in the averaged potentiation and depression can be amplified by employing harder synaptic bounds ($p = 20$). Hard synaptic bounds become only effective if the synaptic weight reaches either the upper or the lower bound so that the weights can evolve freely as long as they stay well within these bounds.

5 Discussion

We have developed a general framework to describe spike-timing dependent synaptic plasticity (STDP) and to investigate the resulting weight dynamics. Instead of developing a biophysical model of transmitter release, ligand gated ion channels and intra-cellular ion concentrations, we have employed a purely phenomenological model that boils down changes in the synaptic efficacy to the arrival time of presynaptic spikes and the firing time of postsynaptic action potentials. The evolution of synaptic weights is expressed in terms of a Volterra-like series expansion using integral kernels that describe weight changes as a function of the relative timing of, e.g., pre- and postsynaptic spikes. The shape of these kernels can directly be inferred from experimental results published for various types of neurons by Markram et al. (1997), Lev-Ram et al. (1997), Bi and Poo (1998), and others.

For slowly varying synaptic weights, the dynamics of the mean weight can be solved explicitly. Not surprisingly, the long-term behavior of the synaptic weights is controlled by *spatio-temporal* correlations of pre- and postsynaptic activity. The importance of temporal correlations for the evolution of synaptic weights, however, is not a unique feature of STDP. Temporally asymmetric learning rules for rate-based neurons have been studied extensively in the context of temporal sequence learning; see, e.g., (Herz et al. 1989; Metzger and Lehmann 1990; Abbott and Blum 1996). Moreover, there are no fundamental differences between STDP and a rate-based learning rule that includes a temporal learning window. The advantage of STDP, however, is that it can account naturally for temporal correlations at a time scale that can be shorter than typical interspike intervals. Both paradigms can result in a stabilization of the postsynaptic firing rate (see (Gerstner and Kistler 2002a) in this issue) and can exhibit pattern formation-like phenomena that are due to competition between individual synaptic weights. Competition arises indirectly from the stabilization of the postsynaptic firing rate and the restriction of individual synaptic weights to a finite interval. In particular, competition does not require any additional non-local mechanisms such as a restriction of global resources (Miller and MacKay 1994).

Nevertheless, there is a subtle difference between STDP and a rate-based learning paradigm with an asymmetric learning window. In addition to correlations in the instantaneous firing rates, a single presynaptic spike can affect the postsynaptic firing time in a spiking neuron model; cf. Eq. (16). Spike-spike correlations are of the order of one over the number of postsynaptic potentials required to reach the firing threshold and are thus, in general, small compared to correlations in the instantaneous firing rates. For (quasi-)stationary firing rates the spike-spike correlations can be absorbed in the term that describes presynaptically triggered (non-Hebbian) weight changes and plays a crucial role in the normalization of the postsynaptic firing rate in STDP if only the Hebbian term with the learning window is included (Song et al. 2000). Non-Hebbian contributions to synaptic plasticity, however, are well documented experimentally (Alonso et al. 1990; Nelson et al. 1993; Urban and Barrionuevo 1996; Salin et al. 1996) so that stability conditions given by Song et al. (2000) regarding, e.g., the total area of the learning window, can be relaxed.

The potential computational power of a learning rule that is sensitive to temporal correlations at a short time scale has been demonstrated by a concrete example. Equipped with STDP, a single neuron can selectively strengthen those synapses that reliably transmit precisely timed spikes at the expense of other synapses that deliver spikes with a broad temporal distribution. Such a mechanism is clearly in favor of a temporal code based on individual action potentials for several reasons. First, STDP allow postsynaptic neurons to discern input channels with meaningful information from noisy ones in an unsupervised fashion. Second, STDP can improve the signal-to-noise ratio by sharpening the postsynaptic firing time distribution. This model also allows for a transparent study of the role of firing threshold and synaptic bounds for the final distribution of synaptic weights.

At present we are close to unraveling the complexity of synaptic plasticity and its implications for network dynamics. Different neurons and the plasticity of their synapses have different characteristic properties depending on their function or the system they are part of. A single synapse may require more than a single scalar – its 'weight' – to characterize the transmission properties if dynamic effects such as short-term synaptic plasticity come into play. Hebbian 'long term' effects may alter these dynamic parameters rather than just the amplitude of the postsynaptic potential (Markram and Tsodyks 1996). On top of this, plasticity parameters themselves may be regulated in an activity dependent manner giving rise to what has been termed *meta-plasticity* (Abraham and Bear 1996). Just as with the proper choice of the neuron model – integrate-and-fire versus multi-compartment – we have to decide what degree of complexity we need and are willing to accept for theory and simulation.

References

Abbott LF, Blum KI (1996) Functional significance of long-term potentiation for sequence learning and prediction. Cerebral Cortex 6: 406–416

Abraham WC, Bear MF (1996) Metaplasticity: the plasticity of synaptic plasticity.Trends Neurosci 19: 126–130

Alonso A, de Curtis M, Llinás R (1990) Postsynaptic Hebbian and non-Hebbian long-term potentiation of synaptic efficacy in the entorhinal cortex in slices and in the isolated adult guinea pig brain. Proc Natl Acad Sci USA 87: 9280–9284

Bartlett MS (1963) The spectral analysis of point processes. JR Statist Soc B 25: 264–296

Bell CC, Han VZ, Sugawara Y, Grant K (1997) Synaptic plasticity in a cerebellum-like structure depends on temporal order. Nature 387: 278–281

Bi G, Poo M (1998) Synaptic modifications in cultured hippocampal neurons: dependence on spike timing, synaptic strength, and postsynaptic cell type. J Neurosci 18: 10464–10472

Bliss TV, Lomo T (1970) Plasticity in a monosynaptic cortical pathway. J Physiol 207: 61P

Bliss TVP, Collingridge GL (1993) A synaptic model of memory: long-term potentiation in the hippocampus. Nature 361: 31–39

Carr CE (1993) Processing of temporal information in the brain. Annu Rev Neurosci 16: 223–243

Cox DR (1955) Some statistical methods connected with series of events. JR Statist Soc B 17: 129–164

Daniel H, Levenes C, Crépel F (1998) Cellular mechanisms of cerebellar LTD. Trends Neurosci 21: 401–407

Denk W, Sigimori M, Llinás R (1995) Two types of calcium response limited to singlespines in cerebellar Purkinje cells. Proc Natl Acad Sci USA 92: 8279–8282

Gerstner W, Abbott LF (1997) Learning navigational maps through potentiation and modulation of hippocampal place cells. J Comput Neurosci 4: 79–94

Gerstner W, Kempter R, van Hemmen JL, Wagner H (1996) A neuronal learning rule for sub-millisecond temporal coding. Nature 384: 76–78

Gerstner W, Kistler WM (2002a) Mathematical formulations of Hebbian learning. Biol Cybern (in press)

Gerstner W, Kistler WM (2002b) Spiking neuron models: Single neurons, populations, plasticity. Cambridge University Press, Cambridge, UK

Gerstner W, van Hemmen JL (1992) Associative memory in a network of 'spiking' neurons. Netw 3: 139–164

Gerstner W, van Hemmen JL (1994) Coding and information processing in neural networks. In: Domany E, van Hemmen JL, Schulten K (eds) Models of Neural Networks II, Springer, New York

Hebb DO (1949) The organization of behavior. Wiley, New York

Herz AVM, Sulzer B, Kühn R, van Hemmen JL (1989) Hebbian learning reconsidered: representation of static and dynamic objects in associative neural nets. Biol Cybern 60: 457–467

Hirano T (1991) Synaptic formations and modulations of synaptic transmissions between identified cerebellar neurons in culture. J Physiol 85: 145–153

Ito M (1984) The cerebellum and neural control Raven Press, New York

Ito M, Kano M (1982)Long-lasting depression of parallel fiber-Purkinje cell transmission induced by conjunctive stimulation of parallel fibers and climbing fibers in the cerebellar cortex. Neurosci Lett 33: 253–258

Karachot L, Kado RT, Ito M (1994) Stimulus parameters for induction of long-term depression in vitro rat Purkinje cells. Neurosci Res 21: 161–168

Kempter R, Gerstner W, van Hemmen JL (1999) Hebbian learning and spiking neurons. Phys Rev E 59: 4498–4514

Kistler WM, Gerstner W, van Hemmen JL (1997) Reduction of the Hodgkin-Huxley equations to a single-variable threshold model. Neural Comput 9: 1015–1045

Kistler WM, van Hemmen JL (1999) Delayed reverberation through time windows as a key to cerebellar function. Biol Cybern 81: 373–380

Kistler WM, van Hemmen JL (2000) Modeling synaptic plasticity in conjunction with the timing of pre- and postsynaptic action potentials. Neural Comput 12: 385–405

Kistler WM, van Hemmen JL, De Zeeuw CI (2000) Time window control: A model for cerebellar function based on synchronization, reverberation, and time slicing. Progr Brain Res 124: 275–297

Konnerth A, Eilers J (1994) Synaptic plasticity and calcium dynamics in cerebellar Purkinje neurons. Biomed Res Supplement 1, 15: 73–77

Lev-Ram V, Jiang T, Wood J, Lawrence DS, Tsien RY (1997) Synergies and coincidence requirements between NO, cGMP, and Ca^{++} in the induction of cerebellar long-term depression. Neuron 18: 1025–1038

Linden DJ (1999) The return of the spike: postsynaptic action potentials and the induction of LTP and LTD. Neuron 22: 661–666

Markram H, Lübke J, Frotscher M, Sakmann B (1997) Regulation of synaptic efficacy by coincidence of postsynaptic APs and EPSPs. Science 275: 213–215

Markram H, Tsodyks M (1996) Redistribution of synaptic efficacy between neocortical pyramidal neurons. Nature 382: 807–810

Mehta MR, Quirk MC, Wilson MW (2000) Experience-dependent asymmetric shape of hippocampal receptive fields. Neuron 25: 707–715

Metzger Y, Lehmann D (1990) Learning temporal sequences by local synaptic changes. Network: Comput Neural Syst 1: 169–188

Miller KD, MacKay DJC (1994) The role of constraints in Hebbian learning. Neural Comput 6: 100–126

Nelson PG, Fields RD, Yu C, Liu Y (1993) Synapse elimination from the mouse neuromuscular junction in vitro: a non-Hebbian activity-dependent process. J Neurobiol 24: 1517–1530

Ngezahayo A, Schachner M, Artola A (2000) Synaptic activity modulates the induction of bidirectional synaptic changes in adult mouse hippocampus. J Neurosci 20: 2451–2458

Salin PA, Malenka RC, Nicoll RA (1996) Cyclic AMP mediates a presynaptic form of LTP at cerebellar parallel fiber synapses. Neuron 16: 797–803

Schreurs BG, Oh MM, Alkon DL (1996) Pairing-specific long-term depression of Purkinje cell excitatory postsynaptic potentials results from a classical conditioning procedure in the rabbit cerebellar slice. J Neurophysiol 75: 1051–1060

Schreurs BG, Tomisc D, Gusev PA, Alkon DA (1997) Dendritic excitability microzones and occluded long-term depression after classical conditioning of the rabbit's nictitating membrane response. J Neurophysiol 77: 86–92

Song S, Miller K, Abbott L (2000) Competitive Hebbian learning through spike-time-dependent synaptic plasticity. Nature Neuroscience 3: 919–926

Urban NN, Barrionuevo G (1996) Induction of Hebbian and non-Hebbian mossy fiber long-term potentiation by distinct patterns of high-frequency stimulation. J Neurosci 16: 4293–4299

van Rossum MCW, Bi GQ, Turrigiano GG (2000) Stable Hebbian learning from spike timing-dependent plasticity. J Neurosci 20: 8812–8821

Wang SS, Denk W, Hausser M (2000) Coincidence detection in single dendritic spines mediated by calcium release. Nat Neurosci 3: 1266–1273